COMMUNICATION

SedNMR: a web tool for optimizing sedimentation of macromolecular solutes for SSNMR

Lucio Ferella · Claudio Luchinat · Enrico Ravera · Antonio Rosato

Abstract We have proposed solid state NMR (SSNMR) of sedimented solutes as a novel approach to sample preparation for biomolecular SSNMR without crystallization or other sample manipulations. The biomolecules are confined by high gravity—obtained by centrifugal forces either directly in a SSNMR rotor or in a ultracentrifugal device—into a hydrated non-crystalline solid suitable for SSNMR investigations. When gravity is removed, the sample reverts to solution and can be treated as any solution NMR sample. We here describe a simple web tool to calculate the relevant parameters for the success of the experiment.

Keywords Ultracentrifuge · Sedimentation · Solid state NMR · Biological macromolecules · Aggregates

Recent advances in theory (Laage et al. 2008; Bertini et al. 2011b; Hu et al. 2011; Loening et al. 2012; Bjerring et al. 2012; Nielsen et al. 2012; Westfeld et al. 2012; Lamley and Lewandowski, 2012; Giffard et al. 2012) and in sample preparation techniques (Lewandowski et al. 2011a; Akbey et al. 2012) have pushed the limits of solid state NMR

L. Ferella · C. Luchinat (✉) · E. Ravera · A. Rosato
Center for Magnetic Resonance (CERM), University of Florence, Via L. Sacconi 6, 50019 Sesto Fiorentino, FI, Italy
e-mail: luchinat@cerm.unifi.it; claudioluchinat@cerm.unifi.it

C. Luchinat
Fondazione Farmacogenomica FiorGen Onlus, Via L. Sacconi 6, 50019 Sesto Fiorentino, FI, Italy

C. Luchinat · E. Ravera · A. Rosato
Department of Chemistry, University of Florence, Via della Lastruccia 3, 50019 Sesto Fiorentino, FI, Italy

(SSNMR) close to that of state-of-the-art solution NMR for the determination of structure (Bertini et al. 2010a; Knight et al. 2011; Luchinat et al. 2012; Huber et al. 2012; Knight et al. 2013; Bhaumik et al. 2013) and dynamics (Lewandowski et al. 2010; Lewandowski et al. 2011b; Knight et al. 2012; Lewandowski 2013; Haller and Schanda, 2013; Schanda et al. 2010; Zinkevich et al. 2013) for micro- to nanocrystalline systems, and even in the case of systems lacking long-range order like fibrils (Petkova et al. 2002; Tycko and Ishii 2003; Debelouchina et al. 2010; Bertini et al. 2011c; Lewandowski et al. 2011a; Bayro et al. 2011; Parthasarathy et al. 2011; Habenstein et al. 2011; Habenstein et al. 2012; Lopez del Amo et al. 2012; Qiang et al. 2012; Lv et al. 2012), large aggregates (Sun et al. 2009; Loquet et al. 2010; Loquet et al. 2012; Byeon et al. 2012; Yan et al. 2013; Loquet et al. 2013), membrane proteins (Ader et al. 2009; Lange et al. 2010; Weingarth and Baldus, 2013; Cady et al. 2010; Hong et al. 2011; Hong 2006; Hong and Schmidt-Rohr 2013; Petkova et al. 2003; Harbison et al. 1985; Marassi and Opella 2000; Opella and Marassi 2004; Marassi et al. 2011; Ding et al. 2013; Opella 2013; Murray et al. 2013; Yang et al. 2011; Hefke et al. 2011; Ullrich and Glaubitz 2013; Ketchem et al. 1993; Sharma et al. 2010) and protein-mineral hybrids (Long et al. 2001; Goobes et al. 2006; Goobes et al. 2007a; Goobes et al. 2007b; Roerich and Drobny 2013; Fragai et al. 2013a). Nevertheless, a wealth of systems still results inaccessible to both solution and solid state NMR.

Very large biomolecular assemblies have solution NMR lines that are broad beyond detection (Wider 2005; Fernández and Wider 2003; Riek et al. 1999; Fiaux et al. 2002; Guo et al. 2008; Tugarinov et al. 2006; Tugarinov et al. 2005a; Tugarinov et al. 2005b; Bermel et al. 2007; Bermel et al. 2008; Bermel et al. 2010). To solve this problem, specific sample preparation and labelling schemes were

Table 1 Parameters for Eqs. 1–3, as given in the web interface

Parameter	Symbol in Eqs. 1–3	Units *	Minimum	Maximum
Molecular weight	M	kDa	1	1,000
Solvent density	$\rho_{solvent}$	g cm^{-3}	0.89 (60 % ethanol)	1.42 (40 % CsCl)
Macromolecular density	$\rho_{biomolecule}$	g cm^{-3}	1.22 (protein)[a]	1.8 (RNA) (Garrett and Grisham 2012)
Starting concentration	c_0	mg cm^{-3}		
Limiting concentration	c_l	mg cm^{-3}	200 (Hyaluronate, MAb, DNAb Helicase)	1,800 (packing of RNA "cubes")
Spinning frequency	(Transformed into ω)	Hz	Maximum spinning rate and inner rotor radius are specified by the producers:	
Inner rotor radius	b	mm	Agilent Technologies and Bruker Biospin	
Temperature	T	K	230 (freezing point of 70 % glycerol water mixture)	373.15 (boiling point of water)

The values are subsequently transformed in SI units

[a] The actual value of the protein density is a debated topic (Andersson and Hovmoller 2000; Quillin and Matthews 2000) We here give the lowest value reported

proposed (Tugarinov et al. 2006; Matzapetakis et al. 2007). Since the lines in SSNMR are independent of the molecular weight of the system, (Marassi et al. 1997) due to the absence of CSA relaxation (Haeberlen and Waugh 1969) [and of Curie-spin relaxation in the case of paramagnetic solids (Kervern et al. 2007)], SSNMR may be considered the technique of choice for atomic-level structural characterization of large biomolecular systems.

In many cases, SSNMR requires the sample to be crystalline and hydrated for obtaining high resolution spectra (Martin and Zilm 2003), but crystal contacts are known to affect in some cases the native structure of the protein (Barbato et al. 1992; Fischer et al. 1999; Skrynnikov et al. 2000; Chou et al. 2001; Poon et al. 2007; Bertini et al. 2008; Bertini et al. 2009). Furthermore, when crystals are obtained, X-ray diffraction gives much simpler access to structural information. Manipulation of the sample (i.e.: precipitation, freezing or lyophilisation) can deteriorate the quality of the spectra (Martin and Zilm 2003; Linden et al. 2011; Pauli et al. 2000; Fragai et al. 2013b).

Mainz et al. proposed that suppressing the rotational diffusion in protein solution could result in a sample that could circumvent the limitations of solution and solid state NMR. This was afforded by "adding glycerol and employing low temperature and high protein concentrations" (Mainz et al. 2009). Indeed, these conditions were shown not to be sufficient to suppress rotational diffusion (Ravera et al. 2013b). Conversely, it has been demonstrated that large macromolecules in solution, sealed in a MAS rotor and spun at the usual MAS NMR frequencies, undergo sedimentation as in a real ultracentrifuge (Bertini et al. 2011d). This can explain the results by (Mainz et al. 2009) and opens the more general opportunity of studying large soluble molecules by SSNMR.

Sedimented solute NMR (SedNMR) (Bertini et al. 2011d; Bertini et al. 2012b; Polenova 2011; Mainz et al. 2012; Gardiennet et al. 2012; Baldwin et al. 2012; Ravera et al. 2013a; Bertini et al. 2013; Luchinat et al. 2013; Mainz et al. 2013) is an ideal tool to address all those soluble biomolecular systems that are too large for solution NMR and that do not crystallize: the sample remains in the buffer used for the solution studies, interactions can be followed like in a usual NMR titration, and the system is always hydrated so as to give highly resolved spectra. The larger the molecules, the easier to obtain them in a good sedimented form.

To foresee the outcome of the SedNMR experiment, we have adapted the usual equation of sedimentation equilibrium (Van Holde and Baldwin 1958) so as to parametrically take into account the pelleting of the macromolecule (Bertini et al. 2011d; Bertini et al. 2012b; Bertini et al. 2012a; Bertini et al. 2013). The macromolecular concentration $c(r)$ at any distance r from the rotation axis of the rotor or of the ultracentrifuge is given by:

$$c(r) = \frac{c_l}{Ae^{-kr^2} + 1}, \tag{1}$$

where c_l is the limiting concentration (see Table 1), k is given by:

$$k = \frac{M(1 - \rho_{solvent}/\rho_{biomolecule})\omega^2}{2RT}, \tag{2}$$

and A is an integration constant that needs to be determined according to the law of conservation of mass. For the geometry of the SSNMR rotor A evaluates analytically to:

$$A = \frac{\exp\left[\frac{M(1-\rho_{solvent}/\rho_{biomolecule})\omega^2 b^2}{2RT}\left(1 - \frac{c_0}{c_l}\right)\right] - 1}{1 - \exp\left[-\frac{M(1-\rho_{solvent}/\rho_{biomolecule})\omega^2 b^2}{2RT}\frac{c_0}{c_l}\right]} \tag{3}$$

As noted elsewhere, the method finds an intrinsic sensitivity limitation in the fact that the starting concentration can optimistically reach 60 % of the corresponding crystal for highly soluble proteins such as BSA (Venturi et al. 2008; Lundh 1980; Lundh 1985;
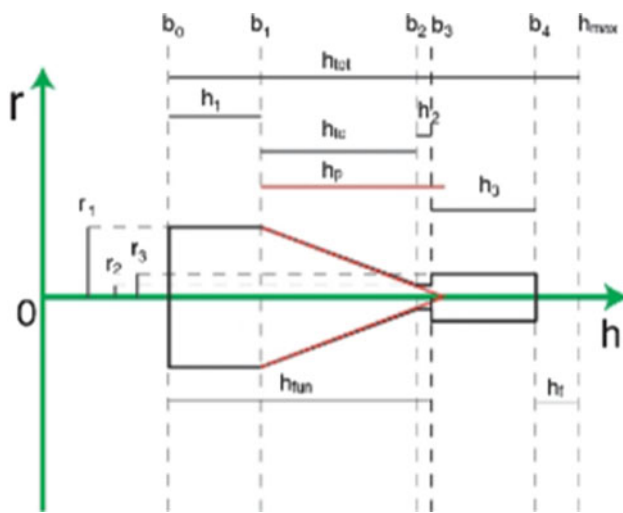
Fig. 1 Schematics of the relevant parameters for the device geometry

Andersson and Hovmoller 2000). Furthermore, the rotors designed for ultra-fast MAS, which can be used to achieve high resolution spectra (Bertini et al. 2010b; Knight et al. 2011; Webber et al. 2012; Asami et al. 2012) and site-specific dynamics information (Lewandowski et al. 2011b; Lewandowski et al. 2010; Schanda et al. 2010; Haller and Schanda 2013), suffer from their small volume and are also penalized by their smaller internal radius that requires higher molecular weights for sedimentation as compared to the other rotors (Bertini et al. 2012b; Bertini et al. 2013).

We thus proposed (Bertini et al. 2012b) that ultracentrifugal devices, like the one described by Böckmann et al. (Böckmann et al. 2009), could be used to form and funnel the sediment directly in the NMR rotor, thus increasing the amount of sample in the rotor. This approach was successfully applied by Gardiennet et al. (Gardiennet et al. 2012) for sedimenting a 59 kDa dodecameric helicase (total molecular weight 708 kDa) and, successively, by Gelis et al. (Gelis et al. 2013) to sediment the ribosome.

In this case, Eqs. 1 and 2 retain their validity, but (Bertini et al. 2012b) the integration constant A needs now to be determined according to the following equation:
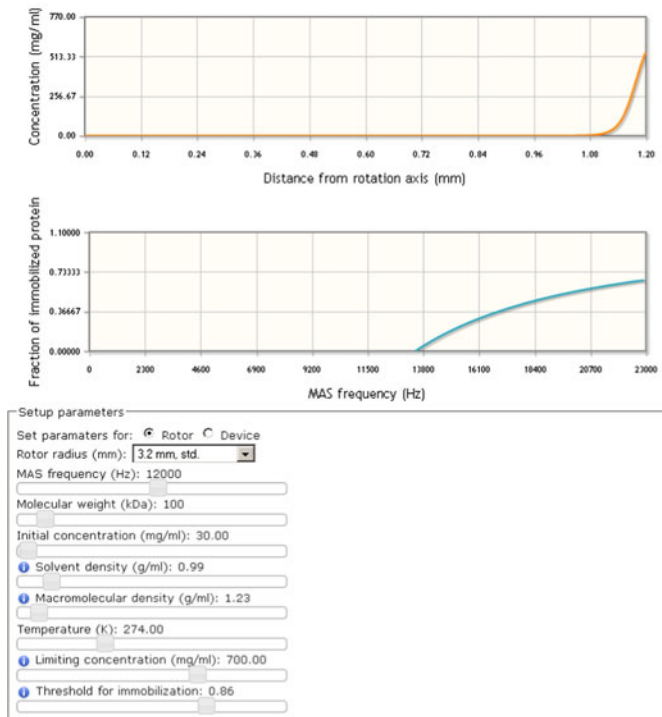

Fig. 2 Appearence of the SedNMR web interface available in WeNMR (http://py-enmr.cerm.unifi.it/access/index/sednmr). The user can tune the parameters using the sliders, according to the properties of the sample under investigation. The graphical output displays the concentration profile as a function of the distance from the rotation axis that would be obtained at a given MAS frequency (*upper panel*) and the fraction of immobilized protein as a function of the MAS frequency for the selected rotors (*lower panel*). The relevant parameters are listed in Table 1, and given with their physically significant range. *Left* "Rotor" option, where calculations are performed for the commercially available Bruker and Agilent rotors. *Right* "Device" option, where the calculations are performed for the device geometry
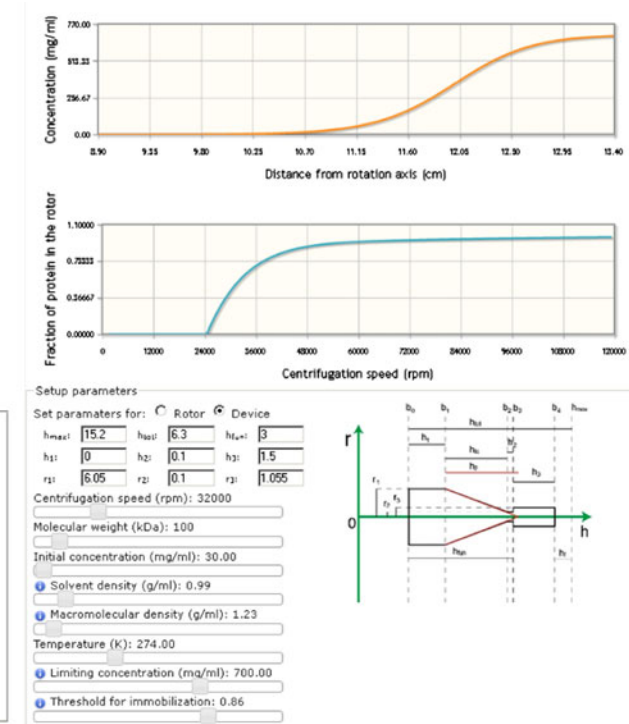
Table 2 Limiting concentrations observed for some biomolecular sediments

ID	Macromolecule	Molecular weight (kDa)	Density[a] (g/ml)	Concentration (g/ml)	References
A	Albumin	66.7	1.24	0.64	(Lundh 1980)
B	Chymotrypsinogen	23.7	1.4	0.72	(Lundh 1980)
C	DNAb Helicase	708	1.23[b]	0.2	(Gardiennet et al. 2012)
D	Ferritin	480	1.23[c]	0.68	(Bertini et al. 2012b)
E	Lysozyme	15	1.59	0.80	(Kennedy and Bryant 1990)
F	Methemoglobin	64.8	1.18	0.73	(Lundh 1985)
G	Monoclonal antibody	150	1.31	0.24	(Rivas and Minton 2011)
H	Transferrin	77	1.31	0.65	(Lundh 1980; Lundh 1985)
I	t-RNA from Baker's yeast	25	1.8[d]	0.8	(Lundh 1980)
J	Ubiquitin	8.6	1.53	0.83	(Fragai et al. 2013b)

[a] Density values are calculated from the molecular weight and the protein volume calculated with the algorithm described in (Voss and Gerstein 2005) and implemented in helixweb.nih.gov/structbio/basic.html

[b] Generic density value as given in (Andersson and Hovmoller 2000)

[c] Experimental value as determined in (Rothen 1944)

[d] Generic density value from (Garrett and Grisham 2012)

Table 3 Fraction of immobilized protein, starting from a 150 mg/ml solution at the maximum spinning rate for some commercially available rotors

ID	1.2	1.6	2.5	3.2	4	5	1.3	1.9	2.5	3.2	4
A	0.8	0.86	0.87	0.81	0.73	0.7	*0.92*	*0.93*	*0.92*	*0.93*	*0.86*
B	0.34	0.67	0.71	0.58	0.35	0.32	*0.82*	*0.84*	*0.82*	*0.83*	*0.68*
C	0.99	0.94	0.99	0.99	0.99	0.99	*0.99*	*0.99*	*0.99*	*0.99*	*0.99*
D	0.97	0.98	0.98	0.97	0.96	0.95	*0.98*	*0.99*	*0.99*	*0.99*	*0.98*
E	0.36	0.57	0.59	0.41	0.14	0.04	*0.75*	*0.877*	*0.74*	*0.77*	*0.55*
F	0.72	0.81	0.82	0.75	0.62	0.58	*0.89*	*0.90*	*0.89*	*0.90*	*0.80*
G	0.97	0.98	0.98	0.97	0.96	0.96	*0.99*	*0.99*	*0.99*	*0.99*	*0.98*
H	0.94	0.90	0.90	0.86	0.80	0.78	*0.94*	*0.95*	*0.94*	*0.95*	*0.90*
I	0.67	0.78	0.79	0.70	0.50	0.51	*0.87*	*0.88*	*0.87*	*0.88*	*0.77*
J	–	0.16	0.22	–	–	–	*0.52*	*0.55*	*0.53*	*0.55*	*0.13*

Values in roman: Agilent technology, values in italics: Bruker Biospin

$$\pi r_1^2 \int\limits_{b_0}^{b_1} c(h)dh + \pi \int\limits_{b_1}^{b_2} \left(\frac{h_p - h + b_1}{h_p} r_1 \right)^2 c(h)dh$$

$$+ \pi r_2^2 \int\limits_{b_2}^{b_3} c(h)dh + \pi r_3^2 \int\limits_{b_3}^{b_4} c(h)dh = c_0 V_{device} \qquad (4)$$

where the meaning of the parameters r_1, r_2, r_3 and h_p and of the integration limits are shown in Fig. 1. These parameters reflect the geometry of the device described in (Bertini et al. 2012a).

The integrals in Eq. 4 are evaluated with the Romberg method as implemented in SciPy (Oliphant 2007).

We have thus developed a user-friendly web interface, based on a framework (Bertini et al. 2011a) that we developed within the WeNMR project (Wassenaar et al. 2012), that allows for the calculation of the concentration profile as a function of distance from the rotation axis. Its appearance is shown in Fig. 2.

The web tool allows for downloading the plot datapoints in a two-column format (which can be imported into a spreadsheet) for offline visualization of the result. All the corresponding parameters values are provided in the RTF format.

The parameter "Threshold for immobilization" that is used to calculate the fraction of immobilized protein in the "ROTOR" option is set to 86 % to match the experimentally determined profile for sedimented ferritin as a function of the rotation rate.(Bertini et al. 2011d; Bertini et al. 2012b) This value represents the value of concentration at

Table 4 Fraction of immobilized protein, starting from a 150 mg/ml solution at the maximum spinning rate for some commercially available rotors

ID	0.75	1	2.5	3.2	4	3	4 Thin	5 Thin
A	0.81	0.82	0.92	0.90	0.88	*0.93*	*0.82*	*0.79*
B	0.58	0.62	0.83	0.78	0.75	*0.84*	*0.61*	*0.55*
C	0.99	0.99	0.99	0.99	0.99	*0.99*	*0.99*	*0.99*
D	0.98	0.99	0.99	0.99	0.99	*0.99*	*0.98*	*0.98*
E	0.42	0.47	0.76	0.70	0.65	*0.78*	*0.46*	*0.38*
F	0.74	0.46	0.89	0.86	0.84	*0.90*	*0.75*	*0.71*
G	0.98	0.98	0.99	0.99	0.98	*0.99*	*0.97*	*0.97*
H	0.86	0.87	0.94	0.93	0.91	*0.95*	*0.87*	*0.85*
I	0.71	0.73	0.88	0.85	0.83	*0.89*	*0.73*	*0.69*
J	–	0.01	0.56	0.44	0.35	*0.58*	–	–

Values in roman: JEOL, values in italics: Doty scientific

which the self-crowding exerted by the protein molecules in solution on each other is enough to abolish the rotational motions to such an extent that a solid-like signal is observed (i.e. the concentration at which the solute becomes a sediment). This is qualitatively expected to occur if the rotational correlation time is slower than the MAS period, so that the nuclear interactions become mechanically averaged.(Haeberlen and Waugh 1969; Matti Mariq and Waugh 1979) There are several models through which a theoretical or empirical calculation of this value could be performed.(Koenig and Brown 1990; Balbo et al. 2013)

Among the parameters listed in Table 1, the most notable is the limiting concentration. This value ranges from the lowest observed value (200 mg/ml for DNAb Helicase) to the theoretical limit of close packing of cubes. A number of experimental observations are given in Table 2. With the data taken from Table 2 we have used the functionality of the sedNMR web tool (http://py-enmr.cerm.unifi.it/access/index/sednmr) to calculate some example results, as summarized in Tables 3 and 4. In Tables 3 and 4, the fraction of immobilized protein with respect to the total protein in the rotor is presented for commonly used rotors. The protein is supposed to have a concentration of 100 mg/ml, and the rotor is supposed to spin at its maximum allowed spinning rate

References

Ader C, Schneider R, Seider K, Etzkorn M, Becker S, Baldus M (2009) Structural rearrangements of membrane proteins probed by water-edited solid-state NMR spectroscopy. J Am Chem Soc 131:170–176

Akbey Ü, van Rossum B-J, Oschkinat H (2012) Practical aspects of high-sensitivity multidimensional ^{13}C MAS NMR spectroscopy of perdeuterated proteins. J Magn Reson 217:77–85

Andersson KM, Hovmoller S (2000) The protein content in crystals and packing coefficients in different space groups. Acta Crystallogr D Biol Crystallogr 56:789–790

Asami S, Szekely K, Schanda P, Meier BH, Reif B (2012) Optimal degree of protonation for (1)H detection of aliphatic sites in randomly deuterated proteins as a function of the MAS frequency. J Biomol NMR 54:155–168

Balbo J, Mereghetti P, Herten D-P, Wade RC (2013) The shape of protein crowders is a major determinant of protein diffusion. Biophys J 104:1576–1584

Baldwin AJ, Walsh P, Hansen DF, Hilton GR, Benesch JLP, Sharpe S, Kay LE (2012) Probing dynamic conformations of the high-molecular-weight αB-crystallin heat shock protein ensemble by NMR spectroscopy. J Am Chem Soc 134:15343–15350

Barbato G, Ikura M, Kay LE, Pastor RW, Bax A (1992) Backbone dynamics of calmodulin studied by ^{15}N relaxation using inverse detected two-dimensional NMR spectroscopy; the central helix is flexible. Biochemistry 31:5269–5278

Bayro MJ, Debelouchina GT, Eddy MT, Birkett NR, MacPhee CE, Rosay MM, Maas W, Dobson CM, Griffin RG (2011) Intermolecular structure determination of amyloid fibrils with magic-angle spinning and dynamic nuclear polarization NMR. J Am Chem Soc 133:13967–13974

Bermel W, Bertini I, Felli IC, Matzapetakis M, Pierattelli R, Theil EC, Turano P (2007) A method for C$^\alpha$ direct-detection in protonless NMR. J Magn Reson 188:301–310

Bermel W, Felli IC, Kümmerle R, Pierattelli R (2008) ^{13}C direct-detection biomolecular NMR. Concepts Magn Reson 32A:183–200

Bermel W, Bertini I, Felli IC, Peruzzini R, Pierattelli R (2010) Exclusively heteronuclear NMR experiments to obtain structural and dynamic information on proteins. ChemPhysChem 11:689–695

Bertini I, Calderone V, Fragai M, Jaiswal R, Luchinat C, Melikian M, Mylonas E, Svergun D (2008) Evidence of reciprocal reorientation of the catalytic and hemopexin-like domains of full-length MMP-12. J Am Chem Soc 130:7011–7021

Bertini I, Kursula P, Luchinat C, Parigi G, Vahokoski J, Willmans M, Yuan J (2009) Accurate solution structures of proteins from X-ray data and minimal set of NMR data: calmodulin peptide complexes as examples. J Am Chem Soc 131:5134–5144

Bertini I, Bhaumik A, De Paepe G, Griffin RG, Lelli M, Lewandowski JR, Luchinat C (2010a) High-resolution solid-state NMR structure of a 17.6 kDa protein. J Am Chem Soc 132:1032–1040

Bertini I, Emsley L, Lelli M, Luchinat C, Mao J, Pintacuda G (2010b) Ultra-fast MAS solid-state NMR permits extensive 13C and 1H detection in paramagnetic metalloproteins. J Am Chem Soc 132:5558–5559

Bertini I, Case DA, Ferella L, Giachetti A, Rosato A (2011a) A grid-enable web portal for NMR structure refinement with AMBER. Bioinformatics 27:2384–2390

Bertini I, Emsley L, Felli IC, Laage S, Lesage A, Lewandoski DA, Marchetti A, Pierattelli R, Pintacuda G (2011b) High-resolution and sensitivity through-bond correlations in ultra-fast MAS solid-state NMR. Chem Sci 2:345–348

Bertini I, Gonnelli L, Luchinat C, Mao J, Nesi A (2011c) A new structural model Aß40 fibrils. J Am Chem Soc 133:16013–16022

Bertini I, Luchinat C, Parigi G, Ravera E, Reif B, Turano P (2011d) Solid-state NMR of proteins sedimented by ultracentrifugation. Proc Natl Acad Sci USA 108:10396–10399

Bertini I, Engelke F, Gonnelli L, Knott B, Luchinat C, Osen D, Ravera E (2012a) On the use of ultracentrifugal devices for sedimented solute NMR. J Biomol NMR 54:123–127

Bertini I, Engelke F, Luchinat C, Parigi G, Ravera E, Rosa C, Turano P (2012b) NMR properties of sedimented solutes. Phys Chem Chem Phys 14:439–447

Bertini I, Luchinat C, Parigi G, Ravera E (2013) SedNMR: on the edge between solution and solid state NMR. Acc Chem Res 46:2059–2069

Bhaumik A, Luchinat C, Parigi G, Ravera E, Rinaldelli M (2013) NMR crystallography on paramagnetic systems: solved and open issues. Cryst Eng Comm 15:8639–8656

Bjerring M, Paaske B, Oschkinat H, Akbey Ü, Nielsen NC (2012) Rapid solid-state NMR of deuterated proteins by interleaved cross-polarization from ^{1}H and ^{2}H nuclei. J Magn Reson 214:324–328

Böckmann A, Gardiennet C, Verel R, Hunkeler A, Loquet A, Pintacuda G, Emsley L, Meier BH, Lesage A (2009) Characterization of different water pools in solid-state NMR protein samples. J Biomol NMR 45:319–327

Byeon I-JL, Hou G, Han Y, Suiter CL, Ahn J, Jung J, Byeon C-H, Gronenborn AM, Polenova T (2012) Motions on the millisecond time scale and multiple conformations of HIV-1 capsid protein: implications for structural polymorphism of CA assemblies. JACS 134:6455–6466

Cady SD, Schmidt-Rohr K, Wang J, Soto CS, DeGrado WF, Hong M (2010) Structure of the amantadine binding site of influenza M2 proton channels in lipid bilayers. Nature 463:689–692

Chou JJ, Li S, Klee CB, Bax A (2001) Solution structure of Ca2 + calmodulin reveals flexible hand-like properties of its domains. Nat Struct Biol 8:990–997

Debelouchina GT, Platt GW, Bayro MJ, Radford SE, Griffin RG (2010) Magic angle spinning NMR analysis of beta(2)-microglobulin amyloid fibrils in two distinct morphologies. J Am Chem Soc 132:10414–10423

Ding Y, Yao Y, Marassi FM (2013) Membrane protein structure determination in membrana. Acc Chem Res 46:2182–2190

Fernández C, Wider G (2003) TROSY in NMR studies of the structure and function of large biological macromolecules. Curr Opin Struct Biol 13:570–580

Fiaux J, Bertelsen EB, Horwich AL, Wüthrich K (2002) NMR analysis of a 900 KDa GroEL GROES complex. Nature 418:207–211

Fischer MW, Losonczi JA, Weaver JL, Prestegard JH (1999) Domain orientation and dynamics in multidomain proteins from residual dipolar couplings. Biochemistry 38:9013–9022

Fragai M, Luchinat C, Martelli T, Ravera E, Sagi I, Solomonov I, Udi Y (2013a) SSNMR of biosilica-entrapped enzymes. Chem Commun. doi:10.1039/c3cc46896h

Fragai M, Luchinat C, Parigi G, Ravera E (2013b) Practical considerations over spectral quality in solid state NMR spectroscopy of soluble proteins. J Biomol NMR 57:155–166

Gardiennet C, Schütz AK, Hunkeler A, Kunert B, Terradot L, Böckmann A, Meier BH (2012) A sedimented sample of a 59 kDa dodecameric helicase yields high-resolution solid-state NMR spectra. Angew Chem Int Edition 51:7855–7858

Garrett RH, Grisham CM (2012) Biochemistry, 5th edn. Brooks/Cole, Belmont

Gelis I, Vitzthum V, Dhimole N, Caporini MA, Schedlbauer A, Carnevale D, Connell SR, Fucini P, Bodenhausen G (2013) Solid-state NMR enhanced by dynamic nuclear polarization as a novel tool for ribosome structural biology. J Biomol NMR 56:85–93

Giffard M, Hediger S, Lewandowski JR, Bardet M, Simorre JP, Griffin RG, De Paëpe G (2012) Compensated second-order recoupling: application to third spin assisted recoupling. Phys Chem Chem Phys 14:7246–7255

Goobes G, Goobes R, Schueler-Furman O, Baker D, Stayton PS, Drobny GP (2006) Folding of the C-terminal bacterial binding domain in statherin upon adsorption onto hydroxyapatite crystals. Proc Natl Acad Sci USA 103:16083–16088

Goobes G, Goobes R, Shaw WJ, Gibson JM, Long JR, Raghunathan V, Schueler-Furman O, Popham JM, Baker D, Campbell CT, Stayton PS, Drobny GP (2007a) The structure, dynamics, and energetics of protein adsorption: lessons learned from adsorption of statherin to hydroxyapatite. Magn Reson Chem 45:S32–S47

Goobes G, Stayton PS, Drobny GP (2007b) Solid-state NMR studies of molecular recognition at protein-mineral interfaces. Progr NMR Spectrosc 50:71–85

Guo C, Zhang D, Tugarinov V (2008) An NMR experiment for simultaneous TROSY-based detection of amide and methyl groups in large proteins. J Am Chem Soc 130:10872–10873

Habenstein B, Wasmer C, Bousset L, Sourigues Y, Schutz A, Loquet A, Meier BH, Melki R, Bockmann A (2011) Extensive de novo solid-state NMR assignments of the 33 kDa C-terminal domain of the Ure2 prion. J Biomol NMR 51:235–243

Habenstein B, Bousset L, Sourigues Y, Kabani M, Loquet A, Meier BH, Melki R, Böckmann A (2012) A native-like conformation for the C-terminal domain of the prion Ure2p within its fibrillar form. Angew Chem Int Ed Engl 51:7963–7966

Haeberlen U, Waugh JS (1969) Spin-lattice relaxation in periodically perturbed systems. Phys Rev 185:420–429

Haller JD, Schanda P (2013) Amplitudes and time scales of picosecond-to-microsecond motion in proteins studied by solid-state NMR: a critical evaluation of experimental approaches and application to crystalline ubiquitin. J Biomol NMR. doi:10.1007/s10858-013-9787-x

Harbison GS, Smith SO, Pardoen JA, Courtin JML, Lugtenburg J, Herzfeld J, Mathies RA, Griffin RG (1985) Solid-state carbon-13 NMR detection of a perturbed 6-s-trans chromophore in bacteriorhodopsin. Biochemistry 24:6955–6962

Hefke F, Bagaria A, Reckel S, Ullrich SJ, Dötsch V, Glaubitz C, Güntert P (2011) Optimization of amino acid type-specific ^{13}C and ^{15}N labeling for the backbone assignment of membrane proteins by solution- and solid-state NMR with the UPLABEL algorithm. J Biomol NMR 49:75–84

Hong M (2006) Solid-state NMR studies of the structure, dynamics, and assembly of β-sheet membrane peptides and α-helical membrane proteins with antibiotic activities. Acc Chem Res 39:176–183

Hong M, Schmidt-Rohr K (2013) Magic-angle-spinning NMR techniques for measuring long-range distances in biological macromolecules. Acc Chem Res 46:2154–2163

Hong M, Zhang Y, Hu F (2011) Membrane protein structure and dynamics from NMR spectroscopy. Annu Rev Phys Chem 63:1–24

Hu B, Lafon OTJ, Chen Q, Amoureux J-P (2011) Broad-band homonuclear correlations assisted by ^{1}H irradiation for biomolecules in very high magnetic field at fast and ultra-fast MAS frequencies. J Magn Reson 212:320–329

Huber M, Böckmann A, Hiller S, Meier BH (2012) 4D solid-state NMR for protein structure determination. Phys Chem Chem Phys 14:5239–5246

Kennedy SD, Bryant RG (1990) Structural effects of hydration: studies of Lysozyme by ^{13}C solids NMR. Biopolymers 29:1801–1806

Kervern G, Steuernagel S, Engelke F, Pintacuda G, Emsley L (2007) Absence of Curie relaxation in paramagnetic solids yields long 1H coherence lifetimes. J Am Chem Soc 129:14118–14119

Ketchem RR, Hu W, Cross TA (1993) High-resolution conformation of gramicidin-A in a lipid bilayer by solid-state NMR. Science 261:1457–1460

Knight MJ, Webber AL, Pell AJ, Guerry P, Barbet-Massin E, Bertini I, Felli IC, Gonnelli L, Pierattelli R, Emsley L, Lesage A, Hermann T, Pintacuda G (2011) Fast resonance assignment and fold determination of human superoxide dismutase by high-resolution proton-detected solid state MAS NMR spectroscopy. Angew Chem Int Edition 50:11697–11701

Knight MJ, Pell AJ, Bertini I, Felli IC, Gonnelli L, Pierattelli R, Hermann T, Emsley L, Pintacuda G (2012) Structure and backbone dynamics of a microcrystalline metalloprotein by solid-state NMR. Proc Natl Acad Sci USA 109:11095–11100

Knight MJ, Felli IC, Pierattelli R, Emsley L, Pintacuda G (2013) Magic angle spinning NMR of paramagnetic proteins. Acc Chem Res 46:2108–2116

Koenig SH, Brown RD III (1990) Field-cycling relaxometry of protein solutions and tissue: implications for MRI. Progr NMR Spectrosc 22:487–567

Laage S, Marchetti A, Sein J, Pierattelli R, Sass HJ, Grzesiek S, Lesage A, Pintacuda G, Emsley L (2008) Band-selective ^1H–^{13}C cross-polarization in fast MAS solid-state NMR spectroscopy. J Am Chem Soc 130:17216–17217

Lamley JM, Lewandowski JR (2012) Simultaneous acquisition of homonuclear and heteronuclear long-distance contacts with time-shared third spin assisted recoupling. J Magn Reson 218:30–34

Lange V, Becker-Baldus J, Kunert B, van Rossum BJ, Casagrande F, Engel A, Roske Y, Scheffel FM, Schneider E, Oschkinat H (2010) A MAS NMR study of the bacterial ABC transporter ArtMP. ChemBioChem 11:547–555

Lewandowski JR (2013) Advances in solid-state relaxation methodology for probing site-specific protein dynamics. Acc Chem Res 46:2018–2027

Lewandowski JR, Sein J, Sass HJ, Grzesiek S, Blackledge M, Emsley L (2010) Measurement of site-specific ^{13}C spin-lattice relaxation in a crystalline protein. J Am Chem Soc 132:8252–8254

Lewandowski JR, Dumez JN, Akbey Ü, Franks WT, Emsley L, Oschkinat H (2011a) Enhanced resolution and coherence lifetimes in the solid-state NMR spectroscopy of perdeuterated proteins under ultrafast magic-angle spinning. J Phys Chem Lett 2:2205–2211

Lewandowski JR, Sass HJ, Grzesiek S, Blackledge M, Emsley L (2011b) Site-specific measurement of slow motions in proteins. J Am Chem Soc 133:16762–16765

Linden AH, Franks WT, Akbey Ü, Lange S, van Rossum B-J, Oschkinat H (2011) Cryogenic temperature effects and resolution upon slow cooling of protein preparations in solid state NMR. J Biomol NMR 51:283–292

Loening NM, Bjerring M, Nielsen NC, Oschkinat H (2012) A comparison of NCO and NCA transfer methods for biological solid-state NMR spectroscopy. J Magn Reson 214:81–90

Long JR, Shaw WJ, Stayton PS, Drobny GP (2001) Structure and dynamics of hydrated statherin on hydroxyapatite as determined by solid-state NMR. Biochemistry 40:15451–15455

Lopez del Amo JM, Schmidt M, Fink U, Dasari M, Fändrich M, Reif B (2012) An asymmetric dimer as the basic subunit in Alzheimer's disease amyloid β fibrils. Angew Chem Int Edition Engl 51:6136–6139

Loquet A, Giller K, Becker S, Lange A (2010) Supramolecular interactions probed by (13)C-(13)C solid-state NMR spectroscopy. J Am Chem Soc 132:15164–15166

Loquet A, Sgourakis NG, Gupta R, Giller K, Riedel D, Goosmann C, Griesinger C, Kolbe M, Baker D, Becker S, Lange A (2012) Atomic model of the type III secretion system needle. Nature 486:276–279

Loquet A, Habenstein B, Lange A (2013) Structural investigations of molecular machines by solid-state NMR. Acc Chem Res 46:2070–2079

Luchinat C, Parigi G, Ravera E, Rinaldelli M (2012) Solid state NMR crystallography through paramagnetic restraints. J Am Chem Soc 134:5006–5009

Luchinat C, Parigi G, Ravera E (2013) Water and protein dynamics in sedimented systems: a relaxometric investigation. Chem Phys Chem 14:3156–3161

Lundh S (1980) Concentrated protein solutions in the analytical ultracentrifuge. J Polym Sci Polym Phys Edition 18:1963–1978

Lundh S (1985) Ultracentrifugation of concentrated biopolymer solutions and effect of ascorbate. Arch Biochem Biophys 241:265–274

Lv G, Kumar A, Giller K, Orcellet ML, Riedel D, Fernandez CO, Becker S, Lange A (2012) Structural comparison of mouse and human α-synuclein amyloid fibrils by solid-state NMR. J Mol Biol 420:99–111

Mainz A, Jehle S, van Rossum BJ, Oschkinat H, Reif B (2009) Large protein complexes with extreme rotational correlation times investigated in solution by magic-angle-spinning NMR spectroscopy. J Am Chem Soc 131:15968–15969

Mainz A, Bardiaux B, Kuppler F, Multhaup G, Felli IC, Pierattelli R, Reif B (2012) Structural and mechanistic implications of metal-binding in the small heat-shock protein αB-crystallin. J Biol Chem 287:1128–1138

Mainz A, Religa TL, Sprangers R, Linser R, Kay LE, Reif B (2013) NMR spectroscopy of soluble protein complexes at one mega-dalton and beyond. Angew Chem Int Edition 52:8746–8751

Marassi FM, Opella SJ (2000) A solid-state NMR index of helical membrane protein structure and topology. J Magn Reson 144:150–155

Marassi FM, Ramamoorthy A, Opella SJ (1997) Complete resolution of the solid-state NMR spectrum of a uniformly 15 N-labeled membrane protein in phospholipid bilayers. Proc Natl Acad Sci USA 94:8551–8556

Marassi FM, Das BB, Lu GJ, Nothnagel HJ, Park SH, Son WS, Tian Y, Opella SJ (2011) Structure determination of membrane proteins in five easy pieces. Methods 55:363–369

Martin RW, Zilm KW (2003) Preparation of protein nanocrystals and their characterization by solid state NMR. J Magn Reson 165:162–174

Matti Mariq M, Waugh JS (1979) NMR in rotating solids. J Chem Phys 70:3300–3316

Matzapetakis M, Turano P, Theil EC, Bertini I (2007) ^{13}C-^{13}C NOESY spectra of a 480 kDa protein: solution NMR of ferritin. J Biomol NMR 38:237–242

Murray DT, Das N, Cross TA (2013) Solid state NMR strategy for characterizing native membrane protein structures. Acc Chem Res 46:2172–2181

Nielsen AB, Székely K, Gath J, Ernst M, Nielsen NC, Meier BH (2012) Simultaneous acquisition of PAR and PAIN spectra. J Biomol NMR 52:283–288

Oliphant TE (2007) Python for scientific computing. Comput Sci Eng 9:10–20

Opella SJ (2013) Structure determination of membrane proteins in their native phospholipid bilayer environment by rotationally aligned solid-state NMR spectroscopy. Acc Chem Res 46:2145–2153

Opella SJ, Marassi FM (2004) Structure determination of membrane proteins by NMR spectroscopy. NMR Spectrosc Chem Rev 104:3587–3606

Parthasarathy S, Long F, Miller Y, Xiao Y, McElheny D, Thurber K, Ma B, Nussinov R, Ishii Y (2011) Molecular-level examination of Cu2+ binding structure for amyloid fibrils of 40-residue

Alzheimer's ß by solid-state NMR spectroscopy. J Am Chem Soc 133:3390–3400

Pauli J, van Rossum B, Forster H, de Groot HJ, Oschkinat H (2000) Sample optimization and identification of signal patterns of amino acid side chains in 2D RFDR spectra of the alpha-spectrin SH3 domain. J Magn Reson 143:411–416

Petkova AT, Ishii Y, Balbach JJ, Antzutkin ON, Leapman RD, Delaglio F, Tycko R (2002) A structural model for Alzheimer's beta-amyloid fibrils based on experimental constraints from solid state NMR. Proc Natl Acad Sci USA 99:16742–16747

Petkova AT, Baldus M, Belenky M, Hong M, Griffin RG, Herzfeld J (2003) Backbone and side chain assignment strategies for multiply labeled membrane peptides and proteins in the solid state. J Magn Reson 160:1–12

Polenova T (2011) Protein NMR spectroscopy: spinning into focus. Nat Chem 3:759–760

Poon DKY, Withers SG, McIntosh LP (2007) Direct demonstration of the flexibility of the glycosylated proline-threonine linker in the Cellulomonas fimi xylanase Cex through NMR spectroscopic analysis. J Biol Chem 282:2091–2100

Qiang W, Yau W-M, Luo Y, Mattson MP, Tycko R (2012) Antiparallel β-sheet architecture in Iowa-mutant β-amyloid fibrils. Proc Natl Acad Sci USA 109:4443–4448

Quillin ML, Matthews BW (2000) Accurate calculation of the density of proteins. Acta Cryst D 56:791–794

Ravera E, Corzilius B, Michaelis VK, Rosa C, Griffin RG, Luchinat C, Bertini I (2013a) Dynamic nuclear polarization of sedimented solutes. J Am Chem Soc 135:1641–1644

Ravera E, Parigi G, Mainz A, Religa TL, Reif B, Luchinat C (2013b) Experimental determination of microsecond reorientation correlation times in protein solutions. J Phys Chem B 117:3548–3553

Riek R, Wider G, Pervushin K, Wüthrich K (1999) Polarization transfer by cross-correlated relaxation in solution NMR with very large molecules. Proc Natl Acad Sci USA 96:4918–4923

Rivas G, Minton AP (2011) Beyond the second virial coefficient: sedimentation equilibrium in highly non-ideal solutions. Methods 54:167–174

Roerich A, Drobny GP (2013) Solid-state NMR studies of biomineralization peptides and proteins. Acc Chem Res 46:2136–2144

Rothen A (1944) Ferritin and apoferritin in the ultracentrifuge: studies on the relationship of ferritin and apoferritin; precision measurements of the rates of sedimentation of apoferritin. J Biol Chem 152:679–693

Schanda P, Meier BH, Ernst M (2010) Quantitative analysis of protein backbone dynamics in microcrystalline ubiquitin by solid-state NMR spectroscopy. J Am Chem Soc 132:15957–15967

Sharma M, Yi MG, Dong H, Qin HJ, Peterson E, Busath DD, Zhou HX, Cross TA (2010) Insight into the mechanism of the influenza A proton channel from a structure in a lipid bilayer. Science 330:509–512

Skrynnikov NR, Goto NK, Yang D, Choy W-Y, Tolman JR, Mueller GA, Kay LE (2000) Orienting domains in proteins using dipolar couplings measured by liquid-state NMR: differences in solution and crystal forms of maltodextrin binding protein loaded with β-cyclodextrin. J Mol Biol 295:1265–1273

Sun SJ, Siglin A, Williams JC, Polenova T (2009) Solid-state and solution NMR studies of the CAP-Gly domain of mammalian dynactin and its interaction with microtubules. J Am Chem Soc 131:10113–10126

Tugarinov V, Choy WY, Orekhov VY, Kay LE (2005a) Solution NMR-derived global fold of a monomeric 82-kDa enzyme. Proc Natl Acad Sci USA 102:622–627

Tugarinov V, Kay LE, Ibraghimov I, Orekhov VY (2005b) High-resolution four-dimensional 1H-13C NOE spectroscopy using methyl-TROSY, sparse data acquisition, and multidimensional decomposition. J Am Chem Soc 127:2767–2775

Tugarinov V, Kanelis V, Kay LE (2006) Isotope labeling strategies for the study of high-molecular-weight proteins by solution NMR spectroscopy. Nat Protoc 1:749–754

Tycko R, Ishii Y (2003) Constraints on supramolecular structure in amyloid fibrils from two-dimensional solid-state NMR spectroscopy with uniform isotopic labeling. J Am Chem Soc 125:6606–6607

Ullrich SJ, Glaubitz C (2013) Perspectives in enzymology of membrane proteins by solid-state NMR. Acc Chem Res 46:2164–2171

Van Holde KE, Baldwin RL (1958) Rapid attainment of sedimentation equilibrium. J Phys Chem 62:734–743

Venturi L, Woodward N, Hibberd D, Marighedo N, Gravelle A, Ferrante G, Hills BP (2008) Multidimensional cross-correlation relaxometry of aqueous protein systems. Appl Magn Reson 33:213–234

Voss NR, Gerstein M (2005) Calculation of standard atomic volumes for RNA and comparison with proteins: RNA is packed more tightly. J Mol Biol 346:477–492

Wassenaar TA, van Dijk M, Loureiro-Ferreira N, van der Schot G, de Vries SJ, Schmitz C, van der Zwan J, Boelens R, Giachetti A, Ferella L, Rosato A, Bertini I, Herrmann T, Jonker HRA, Bagaria A, Jaravine V, Guntert P, Schwalbe H, Vranken WF, Doreleijers JF, Vriend G, Vuister GW, Franke D, Kikhney A, Svergun DI, Fogh RH, Ionides J, Laue ED, Spronk C, Jurksa S, Verlato M, Badoer S, Dal Pra S, Mazzucato M, Frizziero E, Bonvin AMJJ (2012) WeNMR: structural biology on the grid. J Grid Comput 10:743–767

Webber AL, Pell AJ, Barbet-Massin E, Knight MJ, Bertini I, Felli IC, Pierattelli R, Emsley L, Lesage A, Pintacuda G (2012) Combination of DQ and ZQ coherences for sensitive through-bond NMR correlation experiments in biosolids under ultra-fast MAS. ChemPhysChem 13:2405–2411

Weingarth M, Baldus M (2013) Solid-state NMR-based approaches for supramolecular structure elucidation. Acc Chem Res 46:2164–2171

Westfeld T, Verel R, Ernst M, Böckmann A, Meier BH (2012) Properties of the DREAM scheme and its optimization for application to proteins. J Biomol NMR 53:103–112

Wider G (2005) NMR techniques used with very large biological macromolecules in solution. Methods Enzymol 394:382–398

Yan S, Suiter CL, Hou G, Zhang H, Polenova T (2013) Probing structure and dynamics of protein assemblies by magic angle spinning NMR spectroscopy. Acc Chem Res 46:2047–2058

Yang J, Aslimovska L, Glaubitz C (2011) Molecular dynamics of proteorhodopsin in lipid bilayers by solid-state NMR. J Am Chem Soc 133:4874–4881

Zinkevich T, Chevelkov V, Reif B, Saalwachter K, Krushelnitsky A (2013) Internal protein dynamics on ps to mus timescales as studied by multi-frequency N solid-state NMR relaxation. J Biomol NMR. doi:10.1007/s10858-013-9782-2